Optimisation and design of new energy-saving concrete self-insulation block

Autori:

Assoc.Prof. **Bashir H. Osman**, PhD. CE
University of Sinnar, Sinnar, Sudan
College of Engineering, Department of Civil Engineering
bashir00@yahoo.com
Corresponding author

Prof. **Zhongfan Chen**, dPhD. CE
Southeast University, China
Key Laboratory of RC&PC Structures of Ministry of Education
101003944@seu.edu.cn
Corresponding author

Adrianna Carroll, MSc. CE
Integrated Building Services Ltd
Nassau, Bahamas
adriannac@gointegrated.com

Abdelrahman Abuserriya, MSc. CE
University of Sinnar, Sinnar, Sudan
College of Engineering, Department of Civil Engineering
engabedsoliman@hotmail.com

Research Paper

Bashir H. Osman, Zhongfan Chen, Adrianna Carroll, Abdelrahman Abuserriya

Optimisation and design of new energy-saving concrete self-insulation block

This study was designed to satisfy the requirements of energy-saving insulation blocks in severely cold regions, with the thermal and mechanical properties and bulk density comprehensively optimised. An optimal block type was obtained, with the necessary parameters provided and further suggestions for improvement proposed. This study investigated the preparation process and material properties of a new energy-saving self-insulation block. Additionally, both thermal performance and compression tests were designed and conducted on the wall, with the compression performance of the brick and the shear resistance of the wall experimentally studied and optimised using ANSYS.

Key words:

energy saving, concrete self-insulation block, thermal and mechanical properties, optimisation

Prethodno priopćenje

Bashir H. Osman, Zhongfan Chen, Adrianna Carroll, Abdelrahman Abuserriya

Optimizacija i projektiranje novog energetski učinkovitog betonskog samoizolirajućeg bloka

Ovaj rad prikazuje zahtjeve koje moraju zadovoljiti izolacijski blokovi koji se koriste za uštedu energije u izuzetno hladnim regijama. Kroz istraživanje su toplinska i mehanička svojstva te gustoća materijala sveobuhvatno optimizirani kako bi se dobio optimalni tip bloka. Prikazani su zahtijevani parametri i predložene daljnje sugestije za poboljšanja. Rad najprije proučava proces pripreme i svojstva materijala novog energetski učinkovitog betonskog samoizolirajućeg bloka. Također, projektira se i zatim provode ispitivanja vezana uz toplinsko ponašanje te tlačna ispitivanja zida. Konačno, ponašanje opeke pod tlačnim opterećenjem i posmična otpornost zida eksperimentalno su proučeni i optimizirani uporabom računalnog programa ANSYS.

Ključne riječi:

ušteda energije, samoizolirajući betonski blok, toplinska i mehanička svojstva, optimizacija

1. Introduction

Concrete self-insulating blocks have several advantages, ranging from energy and soil conservation to waste disposal and environmental protection [1, 2]. Concrete hollow blocks offer better thermal performance, simplified construction, and reduced construction time while also significantly improving thermal and mechanical performance and conserving energy in buildings [3]. The world is moving toward green buildings and green materials, resulting in improved energy efficiency concepts and zero-energy building standards [4-6]. Self-insulating blocks are one of the few novel building materials with the potential to completely revolutionise the construction industry, with transformative implications for developing nations. Many varieties of high-efficiency and energy-saving blocks with insulation materials have been adopted by researchers in recent years, all of which satisfy the required thermal insulation standards [7-14]. With the implementation of China's national policy on energy conservation and emission reduction, building energy conservation has been highly valued by the local authorities and several codes have been established, with expanded goals to minimize the energy and control energy efficiency to establish sustainable environments [15]. Most approaches to producing new energy-saving concrete self-insulating blocks involve using recycled aggregate [1, 16] and other materials [17].

Huizhi Zhang i sur. [18] proučavali su nosivost i pomake zidova Zhang et al. [18] studied the load capacity and displacement of recycled concrete and a self-insulating block masonry wall using the ABAQUS and laboratory tests, with the results indicating that the masonry compression failure was controlled by a mortar or block with a lower compressive strength. Liu et al. [19] used recycled concrete blocks from construction and demolition waste to study insulation performance and conducted a comprehensive experimental analysis, with the results showing that the insulation concrete block meets the relevant standards with ratios of 45 %, 0.15 % and 30 % for aggregates sand, active activator Na_2SO_4, and fly ash which showed best performance.

Zheng et al. [20] used numerical analysis to analyse the heat transfer law in a cold and dry winter region and optimise its design and the heat and moisture coupling process of the block. Their method was based on a common local composite self-insulation block scheme, using recycled ceramic concrete as the matrix material and a graphite polystyrene board as the insulation material. While their results showed that the structure of a staggered hole can improve the insulation capacity of a block to a certain extent, this approach is not suitable for insulation materials with high water absorption.

This study aims to produce a new energy-saving concrete self-insulation block for optimising the mix design to improve the compressive strength, heat transfer, coefficient, and bulk weight.

Figure 1 shows a flowchart of the methodology used in this study. First, a series of experimental and theoretical studies on thermal performance were conducted to design a new type of self-insulating and load-bearing block for rural houses in different regions. In addition, the basic mechanical and seismic properties of the new type of block wall, the design method of the mix proportion of the recycled concrete block (RCB), and the best replacement ratio of recycled aggregate were studied. Furthermore, numerical models were developed using the ANSYS software to predict the behaviour of the specimens using a simplified micromodelling technique. Finally, the perfect dimensions of an energy-saving concrete self-insulation block (ECSB), which has advantages in terms of both its structural and thermal properties, were optimised, as discussed in the following sections.
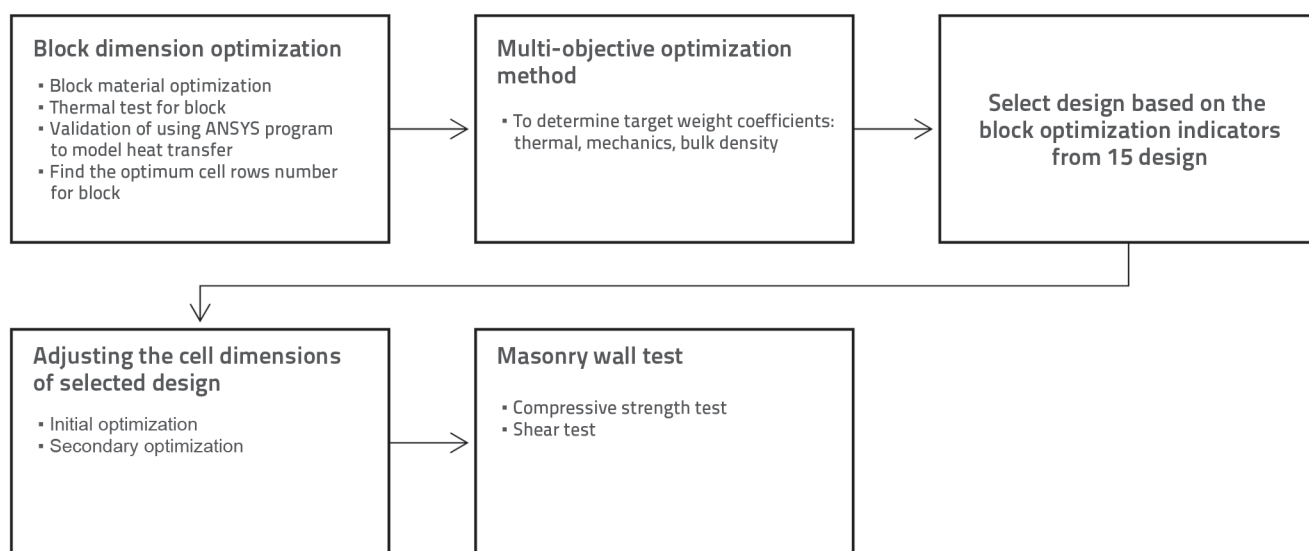

Figure 1. Flow chart of research methodology

2. Design method of new energy-saving concrete self-insulating blocks

2.1. Design principle

Owing to its prospective economic benefits, this new block type is intended for use in low-rise masonry structures in severely cold rural areas. The block can be used to serve as frame structures, shear walls, and infill wall materials in building structures, such as force-wall structures. Based on both the design requirements and China's conditions, block production should not present any difficulty in meeting economic requirements. That is, on the premise of reducing the associated self-weight to facilitate the construction of a more efficient wall, the blocks should be multipurpose and all-in-one with insulation.

Currently, the energy-saving rate for walls in China is approximately 65 % [21]. Some national standards have put forward clear requirements for the heat transfer coefficient of a building's external walls. For example, the Design Criteria for Energy Efficiency of Residential Buildings in Cold Areas [22] recommends that the heat transfer coefficient of the external walls of buildings with 4-8 floors in cold regions (A-zone) according to Chinese climate classification system [23] be limited to 0.4 W/(m2·K), and the "Energy-saving Design Standards for Rural Residential Buildings" [24] recommends that the limit of heat transfer coefficient for exterior walls of residential houses in cold regions be 0.50 W/(m2·K).

China's Technical Specification for High-rise Building Concrete Structures [25] also recommends that the thickness of reinforced walls on the first and second floors and shear walls should not be less than 200 mm, without considering the external wall layer of insulation, implying that the final thickness of the outer wall was at least 280 mm; thus, the block wall thickness was designed to be 280 mm. Decreasing the amount of space in masonry units can improve the overall thermal performance.

2.2. Block material optimization

Small lightweight aggregate concrete hollow blocks, called ceramist concrete hollow blocks, were used in the optimisation process of the current study. The blocks consisted of lightweight aggregates with a bulk density of 1100 kg/m3 and sand, both light and ordinary, with a bulk density of no more than 1950 kg/m3. Based on the raw materials used, ceramsites can be divided into clay, shale, and fly ash and further categorised based on density and strength into: ultra-light ceramsite (bulk density ≤ 500 kg/m3, suitable for the preparation of 5–15 MPa ceramsite concrete), ordinary ceramsite (bulk density ≤ 500–700 kg/m3, suitable for the preparation of 15–35 MPa ceramsite concrete),

and high strength ceramsite (bulk density ≤ 700–900 kg/m3, suitable for the preparation of 30–60 MPa ceramsite concrete)) [26-28].

The ceramsite used in this experiment was clay-based with certain additives. Ceramics are naturally porous, and therefore have a high capacity for water absorption (mostly within 1h) [29-31]. Considering high-strength masonry mortar is necessary to improve the masonry shear resistance strength, block–mortar compatibility will be the focus of subsequent sections.

2.3. Mix design

2.3.1. Raw materials

The ceramsite used in this study is shown in Figure 2 and was produced by Nanjing Xingkai New Building Material Co., Ltd. Ceramsite is a high-strength and stable material that satisfies the basic performance requirements for testing based on the lightweight aggregate and test method [32]. The relevant properties of the ceramsite obtained in the laboratory are listed in Table 1 as obtained in the laboratory. Blocks made with ceramisite concrete have a thermal conductivity of 0.53 W/(m2·K) and a corresponding density of 1200 kg/m3. Ceramsite consists of a primary raw material, which can be either basalt or diabase, and an auxiliary material. The raw materials were combined and made into artificial inorganic fibres.

Compared with traditional building insulation materials, rock wool (Figure 2 and 3) has the advantages of low density, low thermal conductivity, Class A fire protection, stable material properties, good safety (non-toxic, no by-products, no pollution, etc.), and other salient advantages [33-36].

With the aid and expertise of the Shihwa block factory, slag and rock wool were mixed into ceramsite concrete according to prescribed proportions, resulting in cost- and energy-efficient blocks with overall improved thermal insulation performance.
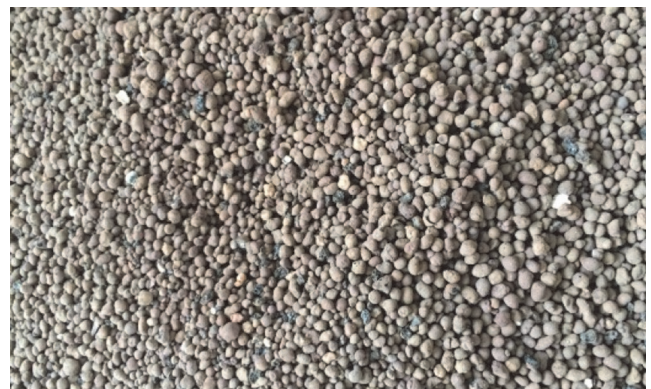

Figure 2. Ceramsite (expanded clay)

Table 1. Basic properties of ceramsite

Bulk density [kg/m3]	Apparent density [kg/m3]	Barrel strength [MPa]	Water absorption [%]	Softening factor [%]
533	720	2.1	8	1

Notably, P.O 42.5 cement manufactured by Nanjing Zhonglian Cement Company meets the requirements of "Universal Portland Cement" [36]. The specific performance parameters are listed in Table 2. Recently, state policies have been introduced to encourage the expansion of the fly ash industry in China. Consequently, research and development into the practical application of fly ash has proven its feasibility in block production. By replacing 10–15 % of the total cement mix with fly ash, blocks were denser owing to a decreased water demand, stronger owing to the pozzolanic reaction of fly ash with lime to produce an additional calcium silicate hydrate binder, allowing the concrete to continue gaining strength over time, and more economical [37, 38].

The fly ash used in the testing, a fine gray powder with a loss on ignition of 3 %, was grade III and produced by a power plant in Nanjing.

Figure 5. 123Block production: a) Plant for forming blocks under pressure; b) Molded products - blocks

According to the seismic design of buildings (DSDB) code, the minimum strength level for load-bearing blocks was set at MU7.5. In rural areas of northern China, most homes are either one or two stories tall. Therefore, in this study, a block strength level of MU5.0.

Reference to "lightweight aggregate concrete technical regulations" [39], which outlines the concrete mix design principles and methods for lightweight aggregates was adhered to during the design phase.

2.4. Production process

A vibration compressive machine for concrete block moulding was designed by the Nanjing Shihwa Block Factory and used in this study. The excitation force in the vibration table was evenly distributed in the mix to ensure the weight, strength consistency, size accuracy, quality, and stability of the product. The preparation process is illustrated in Figure 4. The mechanical equipment and finished block products are shown in Figure 5. After 28 days, the specimens underwent thermal, mechanical, and seismic testing.
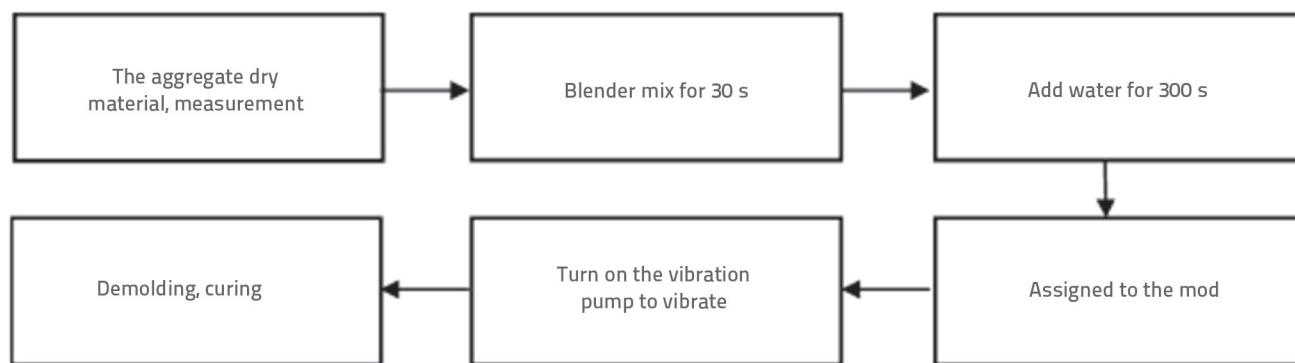

Figure 3. Rock wool

Figure 4. Block preparation process

Table 2. Cement performance parameters

Cement compressive strength [MPa]		Cement flexural strength [MPa]		Standard consistency water consumption [%]	Stability
3 days	28 days	3 days	28 days		
22.3	44.3	4.9	7.3	27	pass

2.5. Thermal performance test

2.5.1. Test Equipment

The hot-box test method was used to gauge the overall thermal performance and thermomechanical properties of the self-insulating block wall. Testing was conducted at Nanjing Jinbi Building Energy Conservation Co., Ltd. (protective hot box for the SK-QB1000B type) and Jiangsu Provincial Construction Engineering Quality Test Centre (Calibrator BC-25), as shown in Figure 6 and 7, respectively.

Figure 6. Protective hot box (SK-QB1000B type)

Figure 7. Calibration Hot Box (Model BC-25)

2.5.2. Thermal test process and results

The outermost cells of the block in the second row lack complete exterior frames, that is, the cells are not completely closed. As such, during the production process, adjacent blocks are butted to form closed cells, with the specific layout shown in Figure 8. Thermal test specimens with dimensions of 390 × 280 × 190 mm were built in

1500 × 1500 mm and 1200 × 1200 mm boxes with a wall thickness of 280 mm. Ordinary mortar was used, and the polystyrene board cell fill was sealed to prevent air and moisture entry. The dried masonry wall primed for thermal testing after 30 d is shown in Figure 9. The areas of the two walls are 1.44 m².
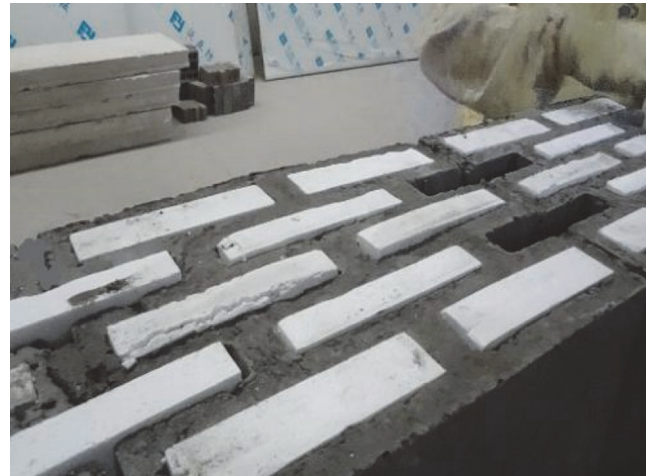

Figure 8. Ash joint cold and hot bridge treatment

Figure 9. Thermal specimen production

After the specimen dried, the hot and cold surfaces on both sides of the wall were uniformly arranged using a temperature sensor. The cold box, hot box, and specimen holder were then closed and the ambient temperature was set for testing. The hot box and cold box temperatures were set to 30 ° C and -15 ° C, respectively. From the test, the resulting heat transfer coefficient of the self-insulation block wall is 0.39 W/(m²·K); meeting the requirements of heat transfer coefficients for cold regions in northeastern China. Cold zones A, B, and C have the following heat transfer coefficient limits; 0.4 W/(m²·K), 0.45 W/(m²·K) and 0.5 W/(m²·K), respectively.

Based on the results, a difference of 0.35 W/(m²·K) was observed between the experimental values obtained and those

values acquired from calculations. Note that the computational values produced represent ideal values; that is, different values obtained through experimentation are expected. Other factors worth considering with regard to the heat transfer coefficient are the environmental humidity and mortar fullness.

2.5.3. Calculation method

This study used the simulation software ANSYS to generate a heat transfer module that covers the heat transfer theory, definition of thermal boundary conditions, model selection, and setting for radiation and natural convection to calculate the thermal performance of the proposed self-insulated blocks. Owing to its multicell irregular configuration, the corresponding three-dimensional block models were established in CAD and later imported to ANSYS for material analysis. The attributes, mesh divisions, and boundary conditions are set. Finally, the temperature load was iteratively calculated to obtain the thermal coefficients of the blocks. Because the temperature fields change over time, thermal analysis can be either a steady-state analysis (the temperature field does not change with time) or a transient analysis (the temperature field changes with time) [40]. As this study considered the steady state, the thermal conductivity of the material is only considered when setting the material properties.

A 360 ×240 × 115 mm composite concrete block with EPS insulation boards was fabricated by the research team. This block considers the thermal conductivities of four different materials, as listed in Table 3. The thermal conductivity was measured using 5 × 5 × 3 mm machined specimens according to GB/T22588-2008 [41] using the Thermal Transport Option (TTO) of the Physical Properties Measurement System (PPMS, Model 6000, Quantum Design, USA). SOLID87 unit, grid size 10 mm, and intelligent free mesh were used for the block model and had the following initial conditions: a heat transfer coefficient of 9.1 W/(m^2·K) for the inner surfaces of the masonry wall, a room temperature of 20 °C, a heat transfer coefficient of 25 W/(m^2·K) for outer surfaces of the masonry wall, and an outdoor temperature of -10 °C [42]. The block modelling and thermal analysis results are shown in Figure 10 and 11, respectively. According to the temperature field distribution results calculated from the block simulation, the heat transfer coefficient is 0.943 W/(m^2·K). The blocks produced in the same batch were tested using calibration and protective hot box methods according to GB/T13475-2008 [43]. The final heat transfer coefficient of the test was 1.038 W/(m^2·K). In addition, ANSYS simulations for recent, relevant, and nationally researched blocks were performed, and their respective thermal performances were evaluated. When the computed thermal performance values obtained from the simulation were compared with the values provided in the literature, the resulting margin of error did not exceed 8 %, thereby verifying the feasibility of using ANSYS to simulate the thermal performance of masonry structures. The simulated and experimental values are listed in Table 4.

Table 3. Block thermal conductivity

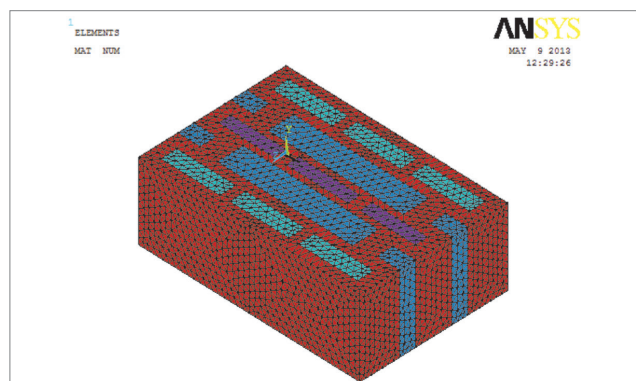| Material	Concrete	EPS	Mort	Air layer	
				20 mm	28 mm
Thermal conductivity [W/ (m·K)]	1,80	0,06	0,87	0,152	0,165

Figure 10. Block model
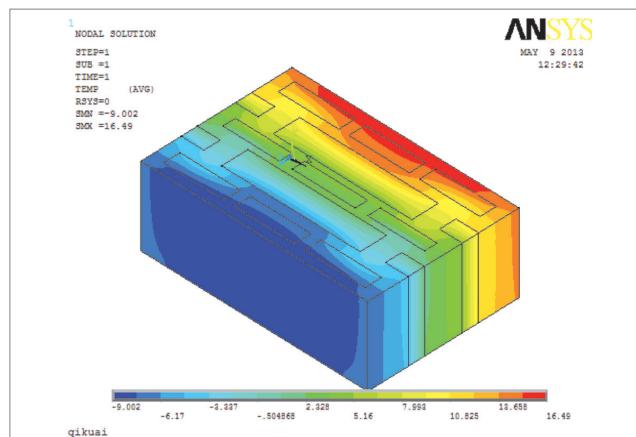
Figure 11. Block temperature analysis results

Table 4. Comparison of simulated heat transfer coefficient of blocks masonry with test results W/(m^2·K)

Block source	Block specifications [mm]	Simulation results	Test results	Error [%]
Sanming [44]	240 × 240 × 90	0.512	0.536	4.48
Huifang [45]	390 × 390 ×190	0.691	0.660	4.70
Hong [46]	390 × 240 ×190	1.312	1.247	5.23
Guangqing [47]	190 × 90 × 90	0.379	0.350	8.29

2.5.4. Principle of calculation

In hollow blocks, heat transfer typically occurs through air in the cells and the ribs around the cells. Therefore, improved cell geometry and material selection would result in improved thermal performance of the self-insulting blocks. The blocks should be designed with multiple rows of misaligned cells, thin-walled ribs, and long convections. The material selected for both the blocks and cell fill should have low thermal conductivity, whereas the fill material should be a thermal insulation material with low thermal conductivity. The overall thermal insulation performance of the block was improved by combining a well-designed cell with high-efficiency insulation.

A comparative study on the effect of evenly and non-uniformly arranged cells in hollow blocks on the heat transfer performance was conducted. Hollow concrete blocks with dimensions of 390 mm × 280 mm × 190 mm were selected and the cell type divided into two groups for analysis: those containing three cell rows and those containing five. The cell size varied accordingly, whereas the hollow rate of the block and the width of the cell ribs were constant. The distribution of the cells in the hollow blocks is shown in Fig. 12. Polyphenylene plates were selected as the filler material based on previous research and were inserted into the cells.

Table 5 shows wall heat transfer coefficients of blocks with different cells.

Table 5. Wall heat transfer coefficients of blocks with different cells

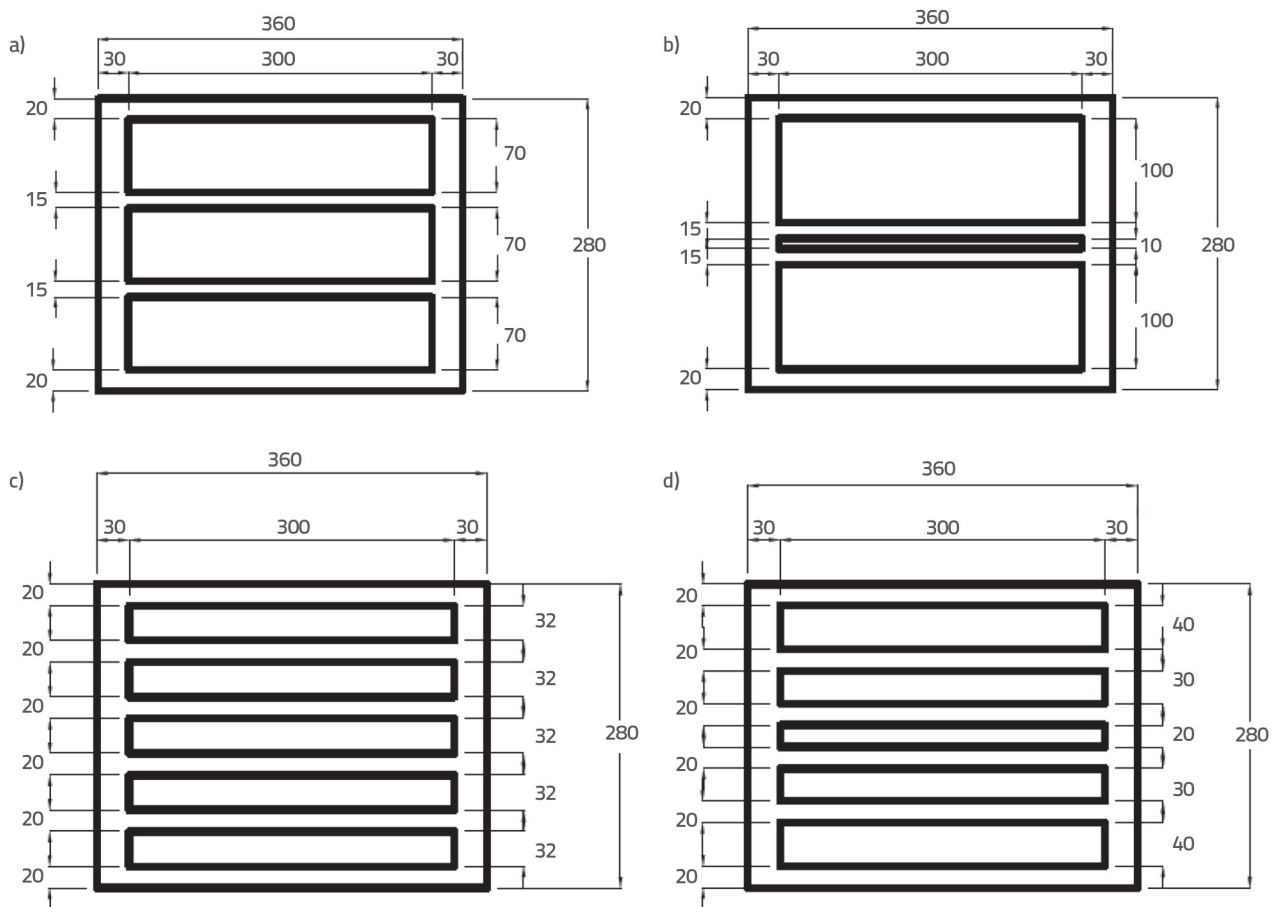| Block specifications	Cell size (in thickness direction) [mm]	Heat transfer coefficient [W/(m²·K)]
Three rows of cells	70+70+70	0.355
	100+10+100	0.347
Five rows of cells	32+32+32+32	0.34
	40+30+20+30+40	0.327

Figure 12. Pore distribution of two groups of blocks

Table 6. Material thermal parameters

Material name	Dry density [kg/m³]	Thermal conductivity [W/(m²·K)]
Ceramsite concrete	1200	0.53
Polystyrene board	500	0.042
Mortar	800	0.29

2.5.5. Selection of wall materials

Initially, cement foam composite aggregates were used as the matrix material for the proposed block, i.e., plastic mortar surrounded by a uniform cement mortar coating. However, a comparative analysis proved that ceramsite concrete was better suited for the current study and was therefore selected as the matrix material for the blocks. Ceramic granules, comprised of various types of clay, slate, shale, coal gangue, and industrial solid waste, has many advantages, such as low density, thermal insulation, excellent impermeability, excellent anti-alkaline aggregate reactivity, low water absorption, good frost resistance, and durability. Using ceramic aggregates instead of coarse aggregates offers several advantages [48].

- Its dry bulk density is 800–1900 kg/m³, (half of the ordinary concrete density), which reduces the weight of the entire building and improves the seismic performance.
- The thermal conductivity is generally lower than that of average concrete by more than half; therefore, the thickness of the wall can be thinned, and the indoor widening correspondingly increases. Under the condition of an equivalent wall thickness, the thermal insulation performance of the room can be significantly improved.

  The surface of ceramsite is rougher than that of gravel and has a certain water absorption capacity. Therefore, the binding ability between the ceramsite and cement mortar is stronger, that is, ceramsite concrete has higher impermeability and durability.
- The fire test results showed that the fire-resistant limit temperature could reach the ordinary one (1.5-2 hours) in more than 3 h.
- Construction has strong adaptability unmatched by other lightweight building materials (such as gas filling) and can be used to formulate different bulk densities and strengths of concrete materials according to the different uses and functions of the building, such as thermal insulation structures or different requirements of load-bearing structures. The thermophysical properties of the tested components were obtained in the laboratory according to the Civil Building Thermal Engineering Design Specifications [23], as listed in Table 6.

2.5.6. Design model

Multiple studies have accredited the best thermal performance among blocks with varying cell geometries to hollow blocks with rectangular cells, followed by blocks with oval cells, and finally those with diamond-shaped or circular cells. Therefore, the cell geometry selected in the block design was rectangular [49, 50]. The block rib wall is designed as a wedge rib with a taper of 2 mm. Additionally, a polystyrene board was used in combination with air layers to reduce the number of polystyrene boards used.

Based on the factors affecting the thermal and mechanical properties of self-insulating blocks, 15 different blocks were designed. The basic block model is shown in Figure 13.

The cells on both sides of the block are symmetrical. Each block consisted of five rows of symmetrical cells on both sides. The thickness between each cell row, called the transverse rib, is the same and is denoted by (f). It is also assumed that the inner wall thickness between each column of cells, called the vertical rib, is the same, and is denoted as (b). The length of the cells in the first row is (a) and has a corresponding width of (e); the cells in the second row are pushed and extended by the vertical ribs, resulting in smaller misaligned cells at either extremity of the block with a length of (x), the functional relationship is 4x+10+2b = 390, and a width of (g).

Determining the thickness of the outer wall (d) of the self-insulating block can be problematic. If the outer wall is too thin, it will lead to nailing failure on the masonry wall, and if the outer wall is too thick, the thermal performance of the wall will be poor. The thickness of the outer wall was set to 20 mm, satisfying the minimum requirement of 15 mm for the outer wall thickness of self-supporting self-insulting concrete composite wall blocks [51]. Most scholars agree that the four corners of self-insulating block cells become circular arcs with a more reasonable force. The optimal arc size was 2 mm, which had little effect on the thermal performance of the blocks. Therefore, in this design, the four corners of the cell are designed as 2 mm arcs.
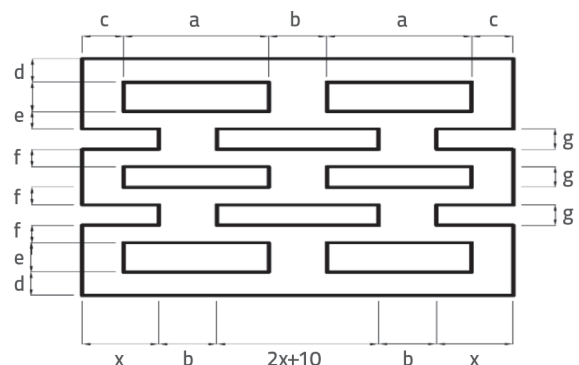

Figure 13. Basic model diagram of self-insulating block

3. New energy-saving concrete self-insulation block type optimization

3.1. Multi-objective optimization principle

The multi-objective optimisation problem can be transformed into a set of objective and constraint functions using a mathematical expression, Eq. (1) [52]:

$$\min_{X\in\Omega} = F(X) = (f_1(X), f_2(X), \ldots, f_m(X)) \tag{1}$$

$X\in\Omega\subset R$ s.t. $g_i(x) \leq 0$; $i = 1, 2, \ldots, p$

Where $X = (X_1, X_1, \ldots, X_n)^T x$ is the n-dimensional space vector, x is the decision space vector of the optimisation target, $i = 1, 2, \ldots, p$ is a function of each target, because each target is x contradictory; that is, not $i = 1, 2, \ldots, p$ simultaneously reaches the minimum value; the m-dimensional space vector $i = 1, 2, \ldots, p$ is the target space, $i = 1, 2, \ldots, p$ is the constraint equation.

3.2. Multi-objective optimization method

Several researchers have conducted in-depth studies on the thermal and mechanical properties of self-insulated concrete blocks [2]. However, the optimisation of their thermal and mechanical properties requires further study. Thermal engineering and mechanics are two phases of block performance, and it is difficult to achieve a uniform optimal solution simultaneously. In this study, a multi-objective optimisation method was used to analyse the thermal performance, mechanical properties, and bulk density of the blocks, and an optimal solution was selected to determine the best block type.

The weighted summation method is a simple, effective, and widely used multi-objective optimisation method. This method builds an objective function according to each goal and obtains the total optimisation function using a weighted summation. The weighted sum of each objective function is 1, the multi-objective optimisation is transformed into a single-objective optimisation, and the mathematical solution is then used to obtain the optimal solution. The mathematical method for weighted summation is shown in Eq. (2) [53]:

$$MiniF\left(X\right) = \sum_{i=1}^{m} w_i f_i\left(x\right) \tag{2}$$

subject to x ∈ Ω

If the weight coefficient is not properly selected, the obtained results are unreasonable, even if the analysis process is rigorous. The weight coefficient in this study was determined using the analytic hierarchy process (AHP) [54], representing a simple, flexible, and practical multicriteria decision-making method for quantifying qualitative questions by establishing and sorting judgment matrices. The core of the AHP is to quantify the judgments of decision makers, enhance the accuracy of the

decision-making basis, and make it more practical in the case of more complex target structures and a lack of statistical data. The analytic hierarchy process (AHP) was used to determine the weights of the evaluation indicators. The index weight coefficients were comprehensively calculated by comparing the relative importance of indicators at the same level.

Three scales (-1, 0, 1) are used to represent the relative importance of each target, i.e., 0 is more important than -1 and 1 is more important than 0. First, self-regulation is used to establish a comparison matrix, which is then converted into a consistency judgment matrix and solved again to obtain the weight values of each target. The specific steps are as follows:

Step 1: The designed blocks are designed to be applied to cold regions in northeast China as infill walls or load-bearing walls for low-rise houses in rural areas. The weight coefficient of each target was determined, demonstrating that thermal performance is more important than mechanical properties. Table 7 establishes the comparison space by setting the thermal performance as P1, the compressive strength as P2, and the bulk density as P3 to obtain the comparison matrix A:

Table 7. Comparison of three factors

Factor	P1	P2	P3
P1	0	1	1
P2	-1	0	1
P3	-1	-1	0

$$A = \begin{bmatrix} 0 & 1 & 1 \\ -1 & 1 & 1 \\ -1 & -1 & 0 \end{bmatrix}$$

Step 2: Solution A, optimal transfer matrix R among them: $r_{ij} = \frac{1}{n}\sum_{k=1}^{n}(a_{ik} + a_{kj})$. Substituting into the comparison matrix A is calculated:

$$R = \begin{bmatrix} 0 & 2/3 & 4/3 \\ -2/3 & 0 & 2/3 \\ -4/3 & -2/3 & 0 \end{bmatrix}$$

Step 3: Transform the matrix R into a consistent matrix D, where: $d_{ij} = \exp(r_{ij})$. Substituting it into:

$$R = \begin{bmatrix} 1 & e^{0.667} & e^{1.333} \\ e^{-0.667} & 1 & e^{0.667} \\ e^{1.333} & e^{-0.667} & 1 \end{bmatrix}$$

Step 4: After comparison matrix A is subjected to the normalisation process described above, its eigenvector is obtained by solving it. Weight coefficient or weighting coefficient of each objective (thermal, mechanical, bulk density) $W_A = [0.563, 0.289, 0.148]^T = (0.563, 0.289, 0.148)$. This weight coefficient can be applied to various types of structures where the strength requirements of the blocks are lower than their thermal indices.

3.3. Standardization of block optimization indicators

Before the weighted summation method can be used for optimisation calculations and analysis, the data must be dimensionless and processed. In this optimisation process, the cell rate is substituted for the bulk density, heat transfer coefficient for the thermal performance, and compressive rate for the mechanical properties. The dimensionless equations are as follows:

$$x_i = 1000 \times p_i/\Sigma p_i \qquad (3)$$

where:

x_i - nondimensional indicators after dimensionless conversion of indicators

p_i - without conversion indicators.

Based on the basic model shown in Fig. 14, 15 different blocks are obtained, as listed in Table 8. The calculation results for the performance indices of each block are listed in Table 9. The width of each cell in the table indicates the thickness along the wall.

3.4. Determining block optimum block type

The evaluation function optimized in this paper is:

$$MaxG(X) = \sum_{i=1}^{3} w_i g_i(x) \sum_{i=1}^{3} w_i = 1$$

where $x \in X$

where $g_i(x)$ is the block heat-transfer coefficient, $g_2(x)$ is the compressive strength of the blocks, $g_3(x)$ is the cell rate of the block. The weight coefficients for each target were calculated as: $w_1 = 0.563$, $w_2 = 0.289$, $w_3 = 0.1483$. The non-dimensional values of the heat transfer coefficient, compressive strength, and bulk of the self-insulating blocks and their corresponding weight coefficients are introduced into the above equation, and the results are listed in Table 10.

As shown in Table 10, block Q3 exhibits the best thermal performance, mechanical properties, and bulk density. The heat transfer coefficient and the compressive strength of the wool cross-section are 0.364 W/(m²·K) and 6.50 MPa, respectively.

Table 8. Different block corresponding block models

Cell width [mm] \ Vertical rib [mm]	20	25	30
36+32+32	Q1	Q2	Q3
39+30+30	Q4	Q5	Q6
48+24+24	Q7	Q8	Q9
54+20+20	Q10	Q11	Q12
60+16+16	Q13	Q14	Q15

Table 9. Dimensionless calculation results of block optimization index

Block name	Heat transfer coefficient [W/(m²·K)]	Heat transfer coefficient (NDV)	Compressive strength [MPa]	Compressive strength (NDV)	Cell rate [kg/m³]	Volume mass (NDV)
Q1	0.346	67.763	6.533	66.697	0.523	68.143
Q2	0.355	69.526	6.540	66.768	0.513	66.840
Q3	0.364	71.289	6.500	66.360	0.502	65.407
Q4	0.342	66.980	6.442	65.768	0.523	68.143
Q5	0.351	68.743	6.543	66.799	0.512	66.710
Q6	0.359	70.309	6.558	66.952	0.502	65.407
Q7	0.330	64.630	6.456	65.911	0.521	67.883
Q8	0.338	66.197	6.543	66.799	0.511	66.580
Q9	0.345	67.568	6.530	66.666	0.501	65.277
Q10	0.324	63.455	6.556	66.931	0.520	67.752
Q11	0.331	64.826	6.584	67.217	0.510	66.450
Q12	0.338	66.197	6.567	67.044	0.501	65.277
Q13	0.321	62.867	6.502	66.380	0.519	67.622
Q14	0.328	64.238	6.578	67.156	0.509	66.319
Q15	0.334	65.413	6.519	66.554	0.508	66.189
Note: NDV denotes non-dimensionalised value						

Table 10. Results of block weighted analysis

Block name	Weighted combined value	Rank
Q1	67.511	5
Q2	68.331	3
Q3	68.994	1
Q4	66.802	7
Q5	67.880	4
Q6	68.613	2
Q7	65.482	12
Q8	66.428	8
Q9	66.968	6
Q10	65.096	14
Q11	65.757	11
Q12	66.306	9
Q13	64.586	15
Q14	65.389	13
Q15	65.858	10

Additionally, the block has a hollow rate of 50 %, a vertical rib thickness of 30 mm, a transverse rib thickness of 18 mm, an outer wall thickness of 20 mm, a total of 5 cell rows, and a thickness of the relevant rib wall size in line with the "self-insulation concrete composite block" [51] requirements. The plane dimensions of block Q3 are shown in Figure 14, the stress calculation cloud diagram is shown in Figure 15, and the maximum rib stresses are listed in Table 10.

3.5. Performance optimization of new energy-saving concrete self-insulating blocks

3.5.1. Initial optimization

The results verify that the optimal thermal performance is obtained when the filled insulation material is closer to both sides of the cold and heat sources. By adjusting the cell dimensions from 36+32+32 to 40+30+30 and reducing the width of the two middle transverse ribs to 17 mm, a preliminary optimised concrete self-insulating block was achieved, the dimensions of which are shown in Figure 16, its stress cloud diagram in Figure 17, and its horizontal and vertical rib maximum stresses in Table 11.
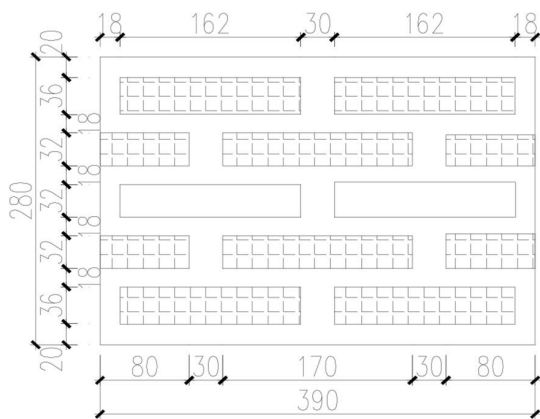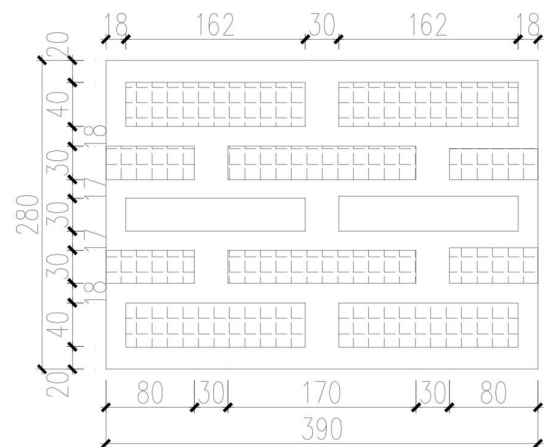

Figure 14. Original plane dimensions of Q3 block

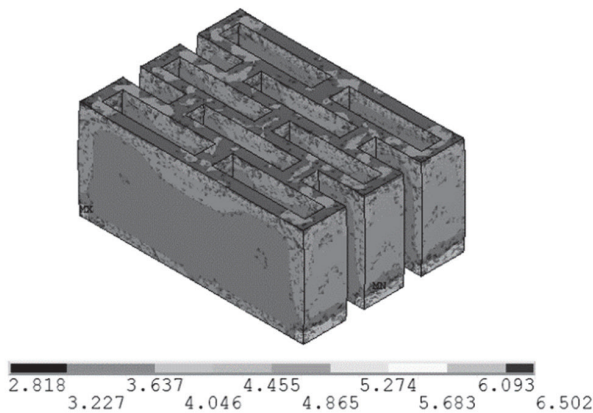**Figure 16. Plane size after initial optimization**

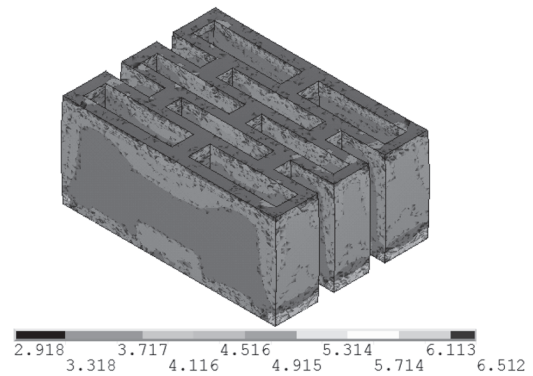**Figure 15. Original stress cloud of Q3 block**

Figure 17. Stress cloud after initial optimization

Table 11. Maximum stress of ribs before and after optimization of Q3 blocks

Rib	Q3 prototype		After initial optimization		After second optimization	
	Thickness [mm]	Maximum stress [MPa]	Thickness [mm]	Maximum stress [MPa]	Thickness [mm]	Maximum stress [MPa]
Cross Rib 1	18	4.257	18	3.85	18	4.848
Cross Rib 2	18	4.837	17	3.667	17	4.860
Vertical rib 1	30	4.911	30	4.798	28	4.797
Vertical rib 2	30	4.557	30	4.605	28	4.653
Vertical rib 3	30	4.882	30	4.873	28	4.655

3.5.2. Secondary optimization

In the first optimisation, the vertical rib thickness was reduced to 28 mm. The changes made to block Q3's dimensions, stress cloud diagram, and maximum stresses are shown in Figures 18, 19, and 11, respectively. The applied boundary and load conditions remained unchanged.

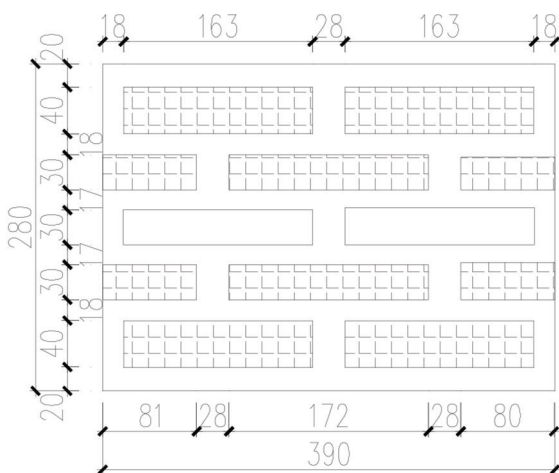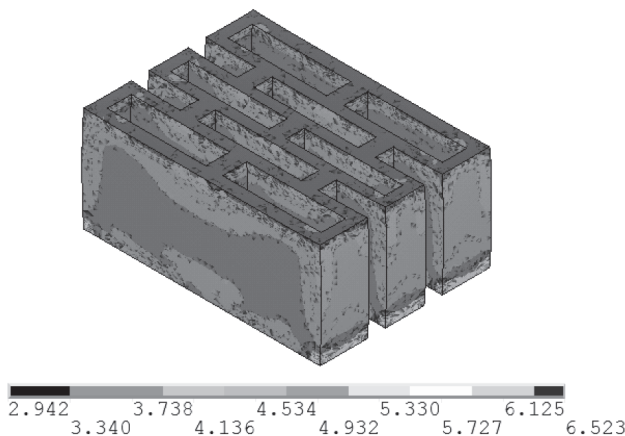**Figure 18. Plane Size after second optimization**

Figure 19. Stress cloud diagram after secondary optimization

When comparing the results from the initial optimisation with those obtained from the second optimisation, it was found that although the horizontal and vertical stress values were similar, the stress distributions were not. It was observed in the stress cloud diagram of the second optimisation that the stress concentration in the pressure plane slowed down, resulting in much lower favourable stresses than those of the preliminary optimisation. Additionally, the reduction in the vertical rib thickness in the second optimisation allowed for redistribution of the stiffness matrix in the vertical ribs.

The second optimisation not only improved the mechanical properties, but also significantly improved the thermal performance. The heat transfer coefficient of the prototype block Q3 was generated by ANSYS and is 0.364 W/(m²·K). After the first optimisation, the heat transfer coefficient lowered to 0.355 W/(m²·K) before further reducing to 0.35 W/(m²·K) in the second optimisation, representing a 3.8 % reduction compared with that of the prototype.

The heat transfer coefficient limits for cold north-eastern regions A, B, and C are 0.4 W/(m²·K), 0.45 W/(m²·K), and 0.5 W/(m²·K), respectively. Block Q3 demonstrated excellent thermal performance after the second optimisation and met both the energy conservation requirements of China for the cold northeastern regions and the development requirements for domestic wall materials. The heat transfer coefficient limits were relaxed in Regions B and C for districts, villages, and towns. In practical applications, the amount of polystyrene board can be reduced according to local conditions, and the board can be flexibly used in different regions. The compressive strength after the second optimisation is 6.5 MPa—suitable for the low-rise masonry structures in villages and towns in China.

By improving both the material quality and production methods, the compressive strength will also improve, ultimately making these blocks suitable for use in load-bearing structures with higher strength requirements.

4. Design of mixture ratio and basic properties of new energy saving self-insulation concrete block

4.1. Specific objectives:

Study the basic mechanical properties (i.e. compressive strength, shear resistance, and cracks development) of masonry block.

Explore compatibility between new energy-saving concrete self-insulation block and mortar.
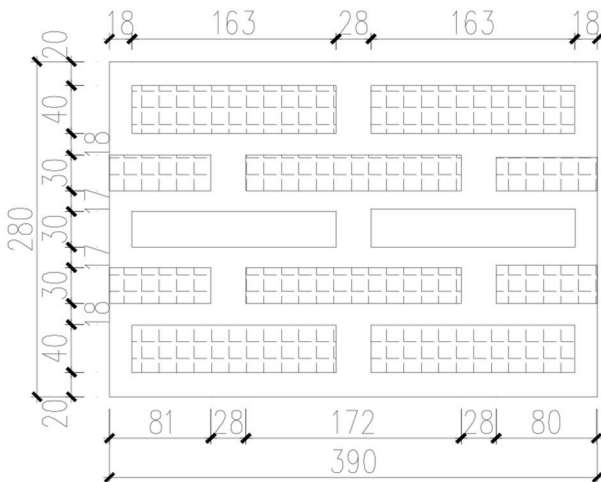

Figure 20. Energy-saving self-insulation block type

4.2. Block and masonry mortar compatibility

4.2.1. Block and mortar compatibility principle

As a general rule of thumb, the "mortar strength will not exceed the brick (block) strength" in masonry structures, based on experimental research conducted over several years. When mortars with different strengths were used, the transverse tensile stress in the block remained virtually unchanged. For example, when the mortar strength was greater than 70 % of the brick strength, the corresponding masonry strength did not increase by more than 10 %. Therefore, it can be deduced that the mortar strength had very little effect on the compressive strength of the masonry unit.

4.2.2. Masonry working mechanism

International and national research agrees that the vertical compressive stress acting on the cross section of a masonry wall unit is an important factor in relation to shear strength, as the shear failure mode is directly determined by vertical compressive stresses. There are three types of shear failure modes for masonry units: shear, shear stress, and baroclinic. However, vertical compressive stresses have a direct impact on the shear strength of masonry units, regardless of the failure mode. Masonry walls are non-homogeneous and composed of blocks held together by a mortar paste.

Because the shear strength along the mortar joints is low in masonry units, mortar should only be used in conjunction with high-strength masonry. In contrast, however, due to the presence of cell openings in hollow blocks, as the strength of the prepared concrete base material is greater than that of the block itself, the strength of the mortar should therefore be compatible with the strength of concrete, as outlined in section 3.5.1 of this paper.

4.3. Masonry pressure performance test

4.3.1. Block and mortar compressive strength

Two groups of blocks with strength grades MU2.5 and MU5 were designed with compressive strengths of 3.06 MPa and 4.45 MPa respectively. The mortar design strength grades were Mb7.5 and Mb10, with measured strengths of 8.7 MPa and 11.5 MPa respectively. Table 12 presents the individual groups and their corresponding strengths. Each group consisted of three specimens, resulting in 12 compressed specimens.

Table 12. Axial compressive specimen assembly puzzle grouping and numbering

Block strength level	Mortar strength grade	
	Mb7.5	**Mb10**
MU2.5	A	B
MU5	C	D

4.3.2. Test setup and loading device

Brick and block test specimens of different sizes required different masonry mechanical properties based on basic test method standards [51]. Per the height ratio β = H/t, β is 3 to 5, and the height of the hollow block masonry wall unit is five block units plus the thickness of the mortar. With a compressive specimen of five units of block masonry, a size of 592 × 280 × 1010 mm, and a thickness of 10 mm in both the horizontal and vertical mortar joints, the resulting height ratio is β = 3.61. The masonry specimens are shown in Figure 21.

Figure 21. Specimen masonry

The test was carried out with a 1000kN hydraulic testing machine at the Civil Engineering College's Structural Laboratory at Southeast University. A compression-testing machine was used to measure the longitudinal and transverse deformations of the specimens. Four dial indicators were arranged symmetrically on both sides, along the vertical and horizontal centrelines. The shear test

Table 13. New composite concrete self-insulating block masonry compression test value

Test piece number	Cracking load [kN]	Failure load [kN]	Cracking load /failure load	Compressive strength [MPa]	Differences [%]
A1	240	420.00	0.57		
A2	290	360.00	0.81	2.36	0.06
A3	340	400.00	0.85		
B1	270	400.00	0.68		
B2	270	410.00	0.66	2.54	0.06
B3	400	460.00	0.87		
C1	330	442.00	0.75		
C2	350	442.00	0.79	2.95	0.14
C3	550	592.00	0.93		
D1	550	715.00	0.77		
D2	540	672.00	0.80	4.1	0.03
D3	530	660.00	0.80		

specimens stood under the pressure plate of the testing apparatus, with its centreline coinciding with the axis of the machine's top and bottom plates. The compression-testing machine and measuring point arrangement are shown in Figure 22.
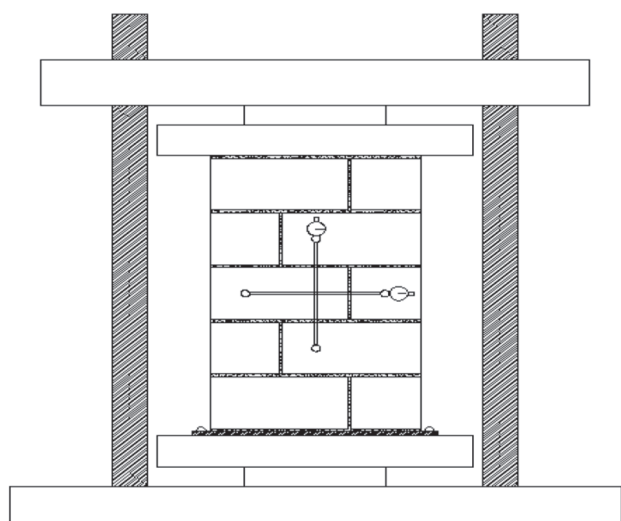

Figure 22. Compression device

Figure 23. Specimen compression damage: a) Broken seams; b) Broken slits

4.3.3. Test phenomenon and results

The specimen underwent three distinct stages when subjected to loading: the elastic stress phase (approximately 50–80 % of the failure load was achieved, indicative of the appearance of cracks), the elastic-plastic stress phase (80 to 90 % of the specimen was destroyed, as seen by crack propagation and development), and the destruction phase (the specimen was instantly crushed and destroyed). The following general observations were made related to the testing process: global brittleness in the test specimens, less concentrated cracks that developed during testing, and the appearance of concentrated cracks that led to early failure. Additionally, it is worth noting that it is relatively easy to produce concentrated stresses when the vertical mortar joints at the top or bottom of the masonry wall unit are in contact with the loading press, and the main cracks are allowed to continuously develop toward the middle of the masonry unit until the longitudinal crack runs through the entire mortar joint bed, as shown in Figure 23.

The compressive strength of the new energy-saving self-insulating concrete block was calculated based on the "basic mechanical properties of the standard masonry test method [51]. The data are summarised in Table 13. In-depth statistics and calculations for the average compressive strength of the specimens and the average compressive strength of lightweight aggregate concrete blocks, based on the Code for Design of Masonry Structures, are listed in Table 14. The values presented in Table 14 indicate that the compressive strength of the new energy-saving self-insulating concrete block is higher than that of its standard lightweight aggregate counterpart. Current Chinese standards provide acceptable formulas that can be used to calculate the average compressive strength of this new concrete block.

Table 14. Axial compressive strength of the measured value and the standard value

Number	Measured value [MPa]	Specification value [MPa]	Measured specification
A	2.36	2.02	1.16
B	2.54	2.24	1.14
C	2.95	2.83	1.04
D	4.10	3.13	1.31

4.3.4. Masonry average compressive strength equation

To use the new type of self-insulating block safely and economically as a viable wall material, an equation to determine the suitable compressive strength is required. Based on the test results, the relevant parameters were corrected using a regression fitting analysis, and the average compressive strength of the new self-insulation block masonry was obtained.

$$lnf_m - \ln(1+0.07)f_2 = lnk_1 + \alpha lnf_1 \tag{4}$$

where:
f_1 - compressive strength of masonry block
f_2 - compressive strength of masonry mortar strength
f_m - compressive strength of masonry wall.

Make $lnf_m - \ln(1+0.07)f_2 = y$, $x = lnf_1$, $a = \alpha$, $b = lnk_1$
Eq. (4) can be transformed into a linear function:

$$y = ax + b \tag{5}$$

The influencing factors related to the block type and masonry method were obtained through a regression fitting analysis of the relevant parameters.

$k_1 = 0{,}72$, $a = 0{,}61$

The average compressive strength of recycled concrete block masonry:

$$f_m = 0{,}72f^{0.61}(1 + 0{,}07)f_2 \tag{6}$$

The measured values of the compressive specimens in each group were compared with those calculated using Eq. (6), it is evident that the values obtained from the proposed formula are slightly lower than those measured during the testing. The calculated from Eq. (6). The measured compressive strength values are shown in Figure 24.
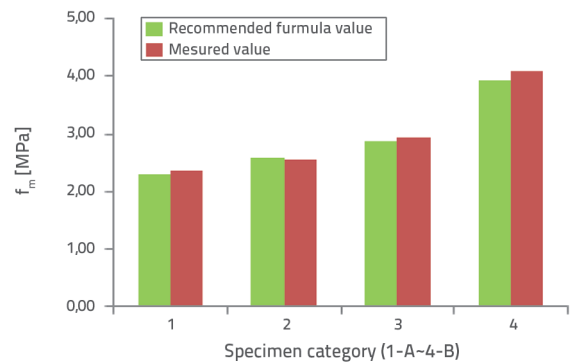

Figure 24. Comparison of the measured values of the compressive strength of the new energy-saving block and the recommended values from formula of Eq. 6

Table 15. Comparison of mortar strength utilization factor with those in the available literature

Source	Group	f_1 [MPa]	f_2 [MPa]	f_m [MPa]	f_1/f_2	$\overline{f_1/f}$	f_2/f_m	$\overline{f_2/f_m}$
Li [31]	1	14.08	6.31	2.23	4.65		2.83	
	2	25.73	6.31	7.55	4.08		0.84	
	3	25.73	15.55	7.92	1.65	2.26	1.96	1.84
	4	31.18	15.55	9.68	2.01		1.61	
	5	31.18	23.26	11.99	1.34		1.94	
Qu [35]	1	27.04	18.90	8.09	1.43		2.34	
	2	33.90	18.90	9.52	1.79		1.99	
	3	40.30	18.90	11.45	2.13	1.60	1.65	2.18
	4	33.90	27.90	9.57	1.22		2.92	
	5	40.30	27.90	13.77	1.44		2.03	
The test presented in this paper	1	3.06	8.67	2.36	0.35		3.67	
	2	3.06	11.48	2.54	0.27		4.52	
	3	4.45	8.67	2.95	0.51	0.38	2.94	3.58
	4	4.45	11.48	4.10	0.39		2.80	

It can be concluded that the proposed equation outlined in this article to calculate the compressive strength of the new energy-saving block is safe and reasonable and has a certain safety reserve for engineering design and application.

Taking the example of a block under axial compression, a complex stress state is generated; the uniaxial compressive strength of the block cannot be effectively utilised owing to the combined effects of the tensile, shear, and bending stresses. The block strength was always higher than the compressive strength of the masonry.

To gain a better perspective on the significance of mortar strength, the ratio of the mortar compressive strength to the masonry compressive strength, called the mortar strength utilisation coefficient, was compared according to the principle of specification compatibility.

It can be seen from Table 15 that the utilization rate of the new mortar block is much higher than that of the ordinary concrete block. The compressive strength of the new-block increased by approximately 60 to 90 % whilst the average mortar strength became 2.68 x higher than that of the average strength of a concrete block.

To guarantee the simultaneous destruction of concrete blocks and mortar, mortar strength should be based on the strength of the concrete block; as specified in the relevant codes. It can therefore be recommended that for high porosity, high strength and high insulation blocks, the mortar strength should be higher than the compressive strength of the block but slightly lower than the strength of a concrete block.

4.4. Masonry shear test

The measured compressive strength values for both blocks and mortar from the same batch, are omitted here. Therefore, the shear properties discussed in this section are purely shear. A 595 × 280 × 600 mm block with a 10 mm mortar joint thickness, as shown in Figure 25, and was designed in accordance with the Standard Test Method for Masonry Basic Mechanical Properties.

Figure 25. Shear test masonry

Figure 26 shows the general experimental setup and Table 16 shows each group with its corresponding strength grades according to GB 50574 [55]. A total of 12 compression specimens were tested; each group contains three specimens.

Figure 26. Shear test device

Table 16. Axial Compression Test Specimens grouped and numbered

Block strength grade	Mortar strength grade	
	Mb7.5	Mb10
MU2,5	AV	BV
MU5	CV	DV

4.4.1. Test process and failure mode results

After reaching their load limit, the specimens experienced a sudden loss in bearing capacity. The main failure occurred at the joint between the mortar and block, but no block failure occurred, as shown in Figure 27, primarily because the mortar layer was restricted to the rib area, which significantly weakened the effective shear area of the block. Although tests typically result in a single shear, the test data summarised in Table 17 consider safety concerns.

The results presented in the table indicate consistent shear strength, a small coefficient of variation, and a higher value of measured shear strength when compared to standard requirements. Consequently, the shear strength of the mortar along the mortar-joint bed is based solely on the strength of the mortar, and the block strength is inconsequential. It can therefore be concluded that the rule of thumb "mortar strength will not exceed the brick strength" that governs standard masonry units does not apply to the proposed energy-saving concrete self-insulation block. For comparison, the pure shear strength equation for existing standard masonry was adopted in the regression of the test data:

$$f_{v,m} = k\sqrt{f_2} \tag{7}$$

Table 17. Shear strength of new self-insulation block masonry section [MPa]

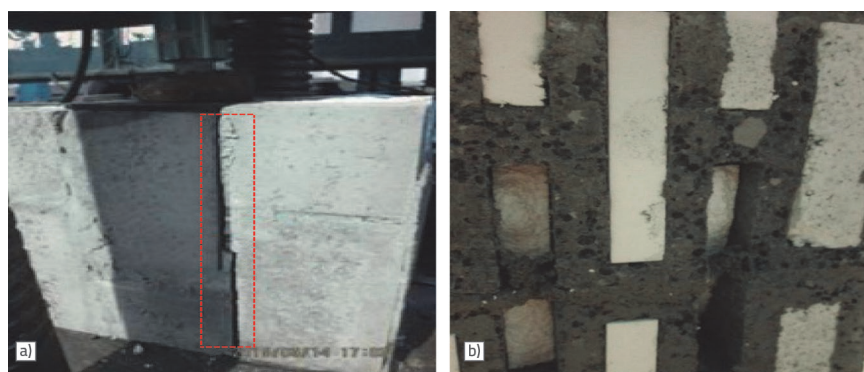| Test piece number	V [kN]	$f_{v.m}$ [MPa]	$\overline{f_{v.m}}$ [MPa]	Coefficient of variation	Standard value	Specification value
AV-1	103.80	0.31				
AV-2	77.13	0.23	0.27	0.13	0.27	0.2
Aas-3	86.00	0.26				
BV-1	113.33	0.34				
BV-2	93.33	0.28	0.30	0.11	0.30	0.2
BV-3	88.60	0.27				
CV-1	106.60	0.31				
CV-2	116.53	0.35	0.36	0.09	0.36	0.23
CV-3	133.80	0.40				
DV-1	126.07	0.38				
DV-2	115.93	0.35	0.36	0.09	0.36	0.23
DV-3	113.8	0.34				

Figure 27. Self-insulation block masonry shear failure mode: a) Single-sided failure; b) Mortar damage to the bonding surface

The least squares method to the measured data regression:
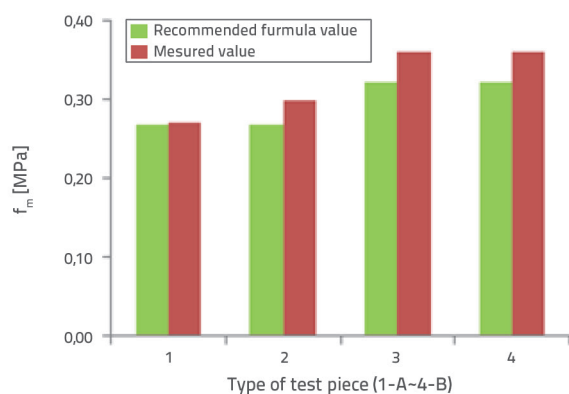
$$f_{v,m} = 0.165\sqrt{f_2} \qquad (8)$$

Figure 28. Comparison of new energy-saving masonry shear strength standard value of the measured value and recommended value from formula of Eq. 8

As shown in Figure 28, the value calculated using Eq. (8) is close to, yet lower than, the measured value. Therefore, using the equation outlined herein to calculate the shear strength of the proposed block is both safe and reasonable.

5. Conclusion

This study investigated the material properties, design parameters, and preparation processes necessary to produce new energy-saving self-insulation blocks for use in severely cold regions, with tests conducted to ascertain their thermal performance, compressive strength, shear resistance, and mortar-block compatibility. The main conclusions are as follows.

- The feasibility of the ANSYS computational method for simulating the thermal performance of the masonry units was verified. As a proposal, under the premise of utilising similar hollow ratios, cells should be arranged in a non-uniform yet symmetrical pattern along the wall perimeter, while the fill should be a thermal insulation material. The insulation of the block proved more effective and more energy-efficient when the fill material was closer to the extremities of the heat and cold sources.
- Considering the influences of thermal engineering, mechanical design factors, and bulk density, a comprehensive multi-objective optimisation analysis was conducted to generate a basic model for a self-insulating energy-saving concrete block, with 15 types of non-inferior block solutions produced. From these 15 solutions, block Q3 was selected, optimised, and analysed using the weighted summation

method. The weight coefficients of each parameter were calculated, and the thermal, mechanical, and bulk weights were 0.563, 0.289, and 0.148, respectively. Overall, block Q3 exhibits superior thermal properties, mechanics, and bulk density.

- Block Q3 was optimised twice. The first optimisation was based on the calculated results from "the concrete block shell and rib thicknesses"; the results indicate that further adjustments to the rib thickness are required. The second optimisation was conducted with an altered rib thickness, yielding satisfactory results: a design for an energy-saving self-insulating block with a thickness of 280 mm. In theory, the heat transfer coefficient of the proposed block wall unit will be lower than that of the standard 0.35 W/(m²·K) heat transfer coefficient limit designated for severely cold regions. The proposed block has dimensions of 390 × 280 × 190 mm, a hollow rate of 50 %, five rows of cells, compressive strength of 6.50 MPa, and rib thickness in accordance with the regulations outlined in JG/T407 [56].

- The heat transfer coefficient of the proposed block is 0.39 W/(m²·K), meeting the energy-saving requirements specified for cold regions.
- For the new energy-saving self-insulation block, the average experimental values for the compressive and shear strengths should be higher than those produced by mathematical computation.
- The unique configuration of the ECSB has advantages in terms of both its structural and thermal properties. Their structural advantage is that they provide stronger bonds than ordinary concrete masonry units by facilitating grout formation between the units. In contrast, the thermal advantage is the reduction in thermal bridges using continuous insulation materials.

Acknowledgments

REFERENCES

[1] Ding, X., et al.: Experimental Study on the Shear Performance of Recycled Concrete Self-Insulating Block Walls. Journal of Materials in Civil Engineering, 33 (2021) 2, pp. 04020456.

[2] Kejkar, R.B., Wanjari, S.P.: Development and optimisation of curing temperature of energy-efficient geopolymer bricks, Građevinar, 72 (2020) 05., pp. 411-420.

[3] Wu, D., et al.: Experimental test for mechanical properties of new tenon composite wall using thermal self-insulation block, Advances in Structural Engineering, 24 (2021) 1, pp. 79-89.

[4] Trkulja, T., Radujković, M., Nikolić-Topalović, M.: Vertical greenery system: a model for improving energy efficiency of buildings, Građevinar, 74 (2022) 07., pp. 561-571, https://doi.org/10.14256/JCE.3370.2021

[5] Hatipoglu, H.K., Cetin, R., Hatipoglu, A.: Sustainable housing: Analysis of energy performance potential in Turkey with translation of building standards of Austria, Građevinar, 74 (2022) 08., pp. 647-659, https://doi.org/10.14256/JCE.3332.2021.

[6] Milovanović, B., Bagarić. M.: How to achieve Nearly zero-energy buildings standard, Građevinar, 72 (2020) 8., pp. 703-720, https://doi.org/10.14256/JCE.2923.2020.

[7] Osman, B.H., Chen, Z.: Experimental Studies on the Behaviors of New Energy-Saving Concrete Self-Insulating Load-Bearing Block Wall under Low-Cycle Cyclic Loading, Advances in Materials Science and Engineering, 2018 (2018), pp. 1-16.

[8] Ding, X., Luo, Y., Chen, Z.: Design and optimization of concrete self-insulation blocks based on thermal and mechanical properties in cold regions, Journal of Southeast University (Natural Science Edition), 45 (2015) 1, pp. 145-150.

[9] Chuan-Meng, Z., De-Hua, D., Guo-Jing, L.: Development and Application of Small Concrete Hollow Blocks, Innovation in Wall Materials and Energy Conservation, 3 (1997), pp. 32-35.

[10] Xiangzhou, L.: Some Trends in the Development of Foreign Wall Materials, Brick and Tile, 7 (2003), pp. 35-36.

[11] Hu, W., et al.: Optimization of the thermal performance of self-insulation hollow blocks under conditions of cold climate and intermittent running of air-conditioning, Case Studies in Thermal Engineering, 35 (2022), pp. 102-148.

[12] Pan, D., et al.: Development of solid waste-based self-insulating material with high strength and low thermal conductivity, Ceramics International, 49 (2023) 3, pp. 5239-5248.

[13] Ali, Y.A., et al.: Use of expanded polystyrene wastes in developing hollow block masonry units, Construction and Building Materials, 241 (2020), pp. 118-149.

[14] Yang, L., et al.: Recent development on heat transfer and various applications of phase-change materials, Journal of Cleaner Production, 287 (2021), pp. 124-432.

[15] National Building Codes Committee, Saudi Building Code Energy Conservation Requirements, 2016, Saudi Building Code, Saudi Arabia.

[16] Guo, Y., et al.: A study on heat transfer performance of recycled aggregate thermal insulation concrete, Journal of Building Engineering, 32 (2020), pp. 101797.

[17] Bai, G.l., et al.: Study on the thermal properties of hollow shale blocks as self-insulating wall materials, Advances in Materials Science and Engineering, 2017 (2017).

[18] Zhang, H., et al.: Load capacity and displacement of recycled concrete and self-insulation block masonry wall. Materials, 13 (2020) 4, pp. 863.

[19] Liu, D., Qiao, L., Li, G.: Experimental Performance Measures of Recycled Insulation Concrete Blocks from Construction and Demolition Waste, J. Renew. Mater, 10 (2022), pp. 1675-1691.

[20] Zheng, W., Song, C., Su,Y.: Analysis and design of coupled heat and moisture performance of new self-insulation blocks of recycled ceramsite concrete, Advances in Frontier Research on Engineering Structures, 1 (2023), CRC Press, pp. 189-198.

[21] Hou, J., et al.: A study on influencing factors of optimum insulation thickness of exterior walls for rural traditional dwellings in northeast of Sichuan hills, China, Case Studies in Construction Materials, 16 (2022), pp. e01033.

[22] 26-2010, J.: Design Standard for Energy Efficiency of Residential Buildings in Cold and Cold Regions, 2010, Architecture & Building Press Beijing, China.

[23] GB50176-93: Thermal Design Specification for Civil Buildings, 1993, China Plan Press Beijing, China.

[24] Ministry of Housing and Urban Rural Development of the People's Republic of China: Design standard for energy efficiency of rural residential buildings (GB/T 50824-2013), China Building Industry Press Beijing, China.

[25] GJ3-2010, T.S.o.: High-rise Building Concrete Structures. 2010, Architecture & Building Press Beijing, China.

[26] Yong-jian, S., Yu-hua, L., Zhi-wen, Y.: Cement-type design of ceramsite concrete block for bearing and heat preservation, Concrete, (2007) 9, pp. 86-87.

[27] Li, Z. Linzhu, S.: The thermal performance analysis of a composite ceramic concrete block with self-thermal insulation, Journal of Hunan University of Technology, 25(2011) 6, pp. 61-65.

[28] Jingwen, W., Tao, J., Shu Rong, L.: Optimized research on the hole type of ceramsite concrete block, New Materials Innovation and Building Energy Conservation, (2009) 4, pp. 32-35.

[29] P., L.L.: Performance test of ceramsite lightweight aggregate concrete and its energy-saving effect analysis, 2015, Zhejiang University.

[30] Xinghui, X., Shuanghui, X.: Experimental and analysis of the compressive strength of clay, Ceramsite and Concrete Small Block Masonry Hui Building, 10 (2003) 3.

[31] Li, W.: Application of ceramsite concrete block masonry, Applied Energy Technology, (1998) 1, pp. 9-10.

[32] T17431.2, G.: Light aggregate and test methods 1998, Standard Press Beijing, China.

[33] Guochang, L., Ping, W.: Preparation and Basic Properties of High-quality Shale Ceramsite Filter, Chinese Journal of Environmental Engineering, 1 (2007) 6, pp. 123-129.

[34] Pingjiang, L., Bo, L.: Basic mechanical properties of high-strength shale ceramsite concrete, Chinese Journal of Building Materials, 7 (2004) 1, pp. 113-116.

[35] Qu, A.: Insulation bearing shale ceramsite small concrete sandwich panels sandwich wall structure. Insulation Materials and Energy Saving Technology, 51 (2004) 4.

[36] GB175-2007: Portland cement. 2007, China Standard Press Beijing, China.

[37] Xiangzhou, L.: Domestic and foreign solid waste management trends and countermeasures, Fly Ash, 16 (2004) 5, pp. 44-47.

[38] Zi-fang, X., Ming-xu, Z., Fan-fei, M.: Analysis of strength mechanism and thermal performance of energy-saving thermal insulation bricks for low temperature firing of solid waste, Chinese Journal of Environmental Engineering, 2 (2008) 4, pp. 548-552.

[39] JGJ51-2002: light aggregate concrete technical specifications, 2002, Building Industry Press Beijing, China.

[40] Jindong, Y.: Analysis of Temperature Field of Reinforced Concrete Structure, Guangdong Building Materials, (2004) 7, pp. 29-31.

[41] GB/T 22588-2008: Determination of thermal diffusivity or thermal conductivity by the flash method, 2008, Standardization Administration of the People's Republic of China.

[42] GB50176-93: Specification for thermal design of civil buildings, 2008, Architecture & Building Press Beijing, China.

[43] GB/T13475-2008: Thermal insulation. Determination of steady-state thermal transmission Properties, Calibrated and guard hot box. 2008, Standardization Administration of the People's Republic of China.

[44] Sanming, Z., Yanping; T.: Thermal performance analysis of different types of concrete perforated brick wall, New Building Materials, (2005).

[45] Huifang, S.: Experimental study on composite self-insulating concrete block masonry, 2010, Zhejiang University of Technology.

[46] Hong, W.: Research on economical energy-saving composite blocks for rural construction, 2010, Yangzhou University.

[47] Guangqing, J.: Die-casting porous bricks, hollow bricks and masonry blocks, World of Tiles, 4 (2009), pp. 9-27.

[48] Wei, Z.: Preparation and Application of Lightweight Aggregate Concrete, 2013, Hunan University.

[49] Bi-chao, Y., Zhou. H.: Thermal Performance Analysis of Concrete Small Hollow Block, in IOP Conference Series: Materials Science and Engineering, 2019. IOP Publishing.

[50] Al-Tamimi, A.S., et al.: Effect of geometry of holes on heat transfer of concrete masonry bricks using numerical analysis, Arabian Journal for Science and Engineering, 42 (2017), pp. 3733-3749.

[51] GBJ50129-2011: Standard for test methods of basic mechanical properties of masonry, 2011, Architecture & Building Press Beijing, China.

[52] Shihong, F., Kewei, D., Yayi, C.: Research on Multi-objective Optimization Method, Journal of Southwest University for Nationalities: Natural Science Edition, 38 (2012) 4, pp. 658-661.

[53] Ma, X., Li, Y., Yan, L.: Comparison review of traditional multi-objective optimization methods and multi-objective genetic algorithm, Electr. Drive Autom, 3 (2010), pp. 48-50.

[54] Yu, P., Wangming, W.: Optimum transfer matrix for antisymmetric, Mathematics in Practice and Recognition, (1988), pp. 61-102.

[55] 50574-2010, G.: Uniform technical code for wall materials used in buildings, 2010, Standardization Administration of the People's Republic of China.

[56] JG/T407-2013: Self-insulated concrete composite block, 2013, Architecture & Building Press Beijing, China.